

# Nonlinear Finite-Element Analysis to Predict Fan-Blade Damage Due to Soft-Body Impact

N. F. Martin Jr.\*

*Pratt & Whitney, West Palm Beach, Florida*

A transient, material and geometric nonlinear, finite-element-based impact analysis, PW/WHAM, is presented. PW/WHAM couples the WHAM program, a transient geometric and material nonlinear plate finite-element analysis, a fluid finite-element projectile, and contact algorithms to form an advanced numerical tool used to predict impact damage on structural components. The impacted component is modeled via WHAM plate finite elements while the impactor may be modeled with WHAM elements (hard-body impact) or fluid finite elements (soft-body impact). The direct integration time marching solution uses the explicit form of the Newmark B-Method difference equations. The spherically shaped fluid finite elements, utilizing a compressible nonlinear fluid constitutive law, are assembled in a closest-packed formation producing the soft-body impactor shape. General contact algorithms continually track the bird/structure interaction eliminating the need for empirical tracking corrections. Several examples demonstrate the excellent correlation with test experience.

## Nomenclature

$A$	= area
$c$	= elastic wave speed
$D$	= distance
$F$	= force
$n$	= number of neighbors
$P$	= pressure
$R_i$	= instantaneous radius
$R_o$	= initial radius
$R_s$	= search radius
$\Delta t$	= time step
$V_i$	= instantaneous volume
$V_o$	= initial volume
$\beta$	= bulk modulus
$\rho$	= density
$\omega$	= natural frequency

## Background

TODAY'S competitive jet engine market requires that engine designs be durable and safe, yet produce ever increasing thrust/weight with the best fuel efficiency. Engine component analytical design tools must be continuously improved in order to achieve these aggressive requirements. Improved design-tool accuracy translates into fewer and more successful engine tests, which reduce both development costs and program delays. Some of the most costly and difficult engine tests involve bird ingestion and fan-blade containment. The ability to predict such damage on fan blades, cases, and supporting structures is essential to minimize development costs. The analytical capability to predict engine-component response to hard- and soft-body impacts is provided by the PW/WHAM program. To predict component damage from birds requires two ingredients: first, a structural model of the component, and second, a method to generate the spatial and temporal distribution of impact loads. The geometric complexities, material nonlinearities, and the component-impactor dynamic interaction make the finite-element (FE) method a

desirable approach. The FE codes such as ADINA, MARC, and WHAM are all capable of predicting the nonlinear structural response when given the correct impact load. WHAM is selected based upon the solution procedure, adaptable code, and initial procurement costs. The challenge is to develop a method to produce accurate impact loads. It is the generation of this impact load via a fluid FE model that makes PW/WHAM a unique program capable of predicting fan-blade response to bird strike.

A projectile is considered a "soft-body" when the internal stresses generated during the impact event substantially exceed the projectile material strength but are far below the target material strength. For this reason, soft-body projectiles are observed to "flow" as a fluid upon impact while the target may be undeformed. The "flow" phenomenon was observed by Hopkins and Kolsky<sup>1</sup> for the impacts of solids. The projectile response was divided into five categories as a function of impact speed: elastic, plastic, hydrodynamic, sonic, or explosive. The internal stresses in the projectile during an elastic impact are well below the material strength. The projectile will rebound based upon the coefficient of restitution. As the impact velocity increases, plastic response of the projectile begins, but the projectile material strength is still sufficient to prevent a fluid-like response. However, further increasing the impact velocity causes internal stresses to exceed the material strength of the projectile and fluid-like flow is observed. At this velocity, the material density, not the material strength, determines the projectile response.

Allcock and Collin<sup>2</sup> studied wax, foam, emulsions, and gelatin as substitute materials for birds. They concluded that the soft-material substitutes with specific gravities of water produced loading profiles similar to birds. These results involving materials of varying strengths indicate that material density, not material strength, was the dominant factor. Barber et al.<sup>3</sup> found that birds impacting a rigid target generated peak pressures which were independent of bird size and proportional to the impact velocity squared indicating that a fluid-like response was occurring. Concerned with soft-body damage on aircraft windshields, Peterson and Barber<sup>4</sup> studied the impact pressures caused by birds on a flat, rigid plate while varying the impact angle and impact velocity. They concluded that 1) birds behave essentially as a fluid during impact, 2) birds do not bounce, and 3) the duration of load is approximately the "squash-up" time. In a later study, Barber et al.<sup>5,6</sup> characterized the soft-body impact as a four-step process: 1) initial shock (Hugoniot), 2) impact shock decay, 3) steady-

Presented as Paper 88-3163 at the AIAA/ASME/SAE/ASEE 24th Joint Propulsion Conference, Boston, MA, July 11-13, 1988; received July 25, 1988; revision received March 31, 1989. Copyright © 1988 American Institute of Aeronautics and Astronautics, Inc. All rights reserved.

\*Technical Specialist, Structures Technologies Group.

state fluid jet flow, and 4) decay. A gelatin material was shown to be a suitable bird substitute.

The first soft-body loading models involved simple average momentum relations.<sup>2,4,6,7</sup> Tsai et al.<sup>7</sup> developed a working deflection-momentum relation for an impacted cantilevered beam. The loads were not interactive with the deflecting beam. Cornell<sup>8</sup> developed a simple fluid-based missile loading model which was interactive with a three-degree-of-freedom fan-blade model. This model was limited to shallow impact angles and small deflections of the target. An improved fluid missile loading model was developed which subdivided the incoming projectile into parallel jets, attempting to account for material spreading and squashing.<sup>9</sup> Fulton<sup>10</sup> introduced a loading model which treated the projectile as an incompressible fluid. This model, although an improvement over the previous formulations, was still limited to small target deflections.

The early applications of the FE technique to the field of dynamic transient problems followed from the static solution which used a stiffness matrix. This stiffness matrix solution was coupled with either an implicit time integration or an explicit time integration procedure.<sup>11-14</sup> As the transient analysis procedure matured, it was discovered that a direct force calculation was more efficient than the traditional stiffness matrix solution. Oden<sup>15,16</sup> was the first to directly solve for the nodal forces in a transient problem including both geometric and material nonlinearities. Others continued the development using explicit and implicit integration procedures, large displacement and large strain relations with either a Eulerian or Lagrangian formulation.<sup>17-19</sup> Krieg and Key<sup>20</sup> concluded that for the transient response problem the conditionally stable explicit central-difference time integration coupled with a lumped mass representation was more efficient than the implicit integration procedure. Belytschko and co-workers<sup>21-24</sup> agreed with this conclusion and developed a transient analysis, WHAM, which included material and geometric nonlinearities. A pseudo-Lagrangian coordinate system, using a convected coordinate approach, was attached to the element. The element coordinate system could undergo larger rotations, but could not deform, hence the analysis was a large-deflection small-strain procedure.

### Fluid Finite Element

An analysis capable of simulating a soft-body impact on a structure must include both geometric and material nonlinearities. The impacting projectile undergoes large deflections and segmentation while interacting with the deforming structure. The goal of the soft-body projectile modeling technique is to generate an approximate spatial and temporal load transfer to the impacted structure. Prediction of the microfluid response of the projectile (such as the Hugoniot pressure peak) is not sought, instead, the goal is to predict the macrofluid response. The fluid-like behavior and the large

deflection requirements of the soft-body impact event are most easily handled by the FE technique. The FE technique subdivides the body to be studied into finite segments or elements. Each fluid element reacts to external loads or deflections through a constitutive law and interacts with other elements based upon the connectivity.

A spherical element is proposed<sup>25</sup> which has a centrally located node, initial radius  $R_o$ , and an initial volume  $V_o$ . The inviscid fluid assumption limits the element to three translational degrees of freedom. The element reacts to external contact by uniformly contracting or expanding. The spherical shape is maintained as the radius varies. Resulting volume changes create internal element pressure via the fluid pressure-volume relationship<sup>26</sup>:

$$P = \beta \ln(V_o/V_i) \quad (1)$$

The internal pressure is converted to a force by defining a contact area. Consider the single element impacting a rigid flat surface, Fig. 1, acting on area  $A$ .

$$A = \pi(R_o^2 - R_i^2) \quad (2)$$

The resulting force  $F$  is

$$F = 3\pi\beta(R_o^2 - R_i^2)\ln(R_o/R_i) \quad (3)$$

This force is applied in equal and opposite directions to the element and the rigid flat surface. The inviscid flow assumption dictates that these forces be normal to the target surface.

The spherical fluid elements are assembled in a closest-packed formation producing the soft-body projectile shape. In three-dimensional space, each interior fluid element is surrounded by 12 nearest neighbors (Fig. 2). The volume between the elements represents lost mass which is included by increasing the initial fluid density of each element until the actual projectile mass and the model mass are equal.

Each element, to maintain continuity of the projectile, must contract or expand. This change in size is determined by an invariant averaging technique involving the distance from the element node to the nearest neighbor nodes (Fig. 3).

$$R_i = (D_1/2 + D_2/2 + \dots + D_n/2)/n \quad (4)$$

Unlike an FE representation of a structure, the fluid element model does not exhibit a fixed connectivity between adjacent elements. The elements are not structurally connected, but are simply in the proximity of other elements. All of the fluid elements defining the projectile are initially of equal size, but as the projectile deforms so must the elements. The deformation changes the relative position and the size of the assembled elements. The determination of which elements are nearest neighbors is limited by the search radius  $R_s$ . The search radius

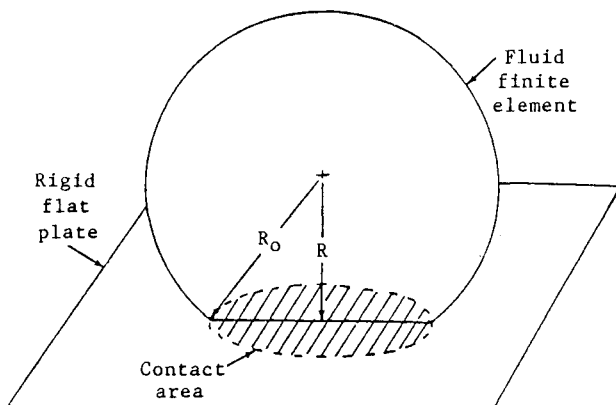


Fig. 1 Fluid element impacting a flat rigid surface.

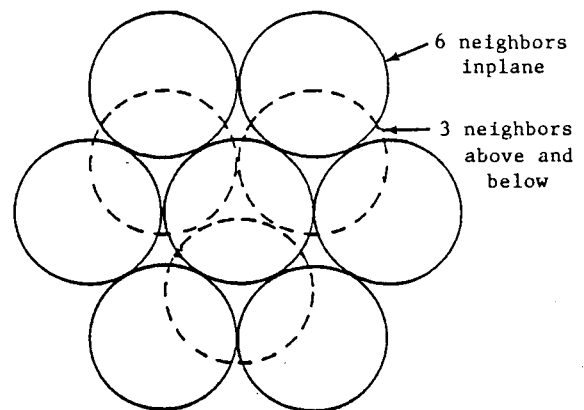


Fig. 2 Closest-packed formation of fluid elements.

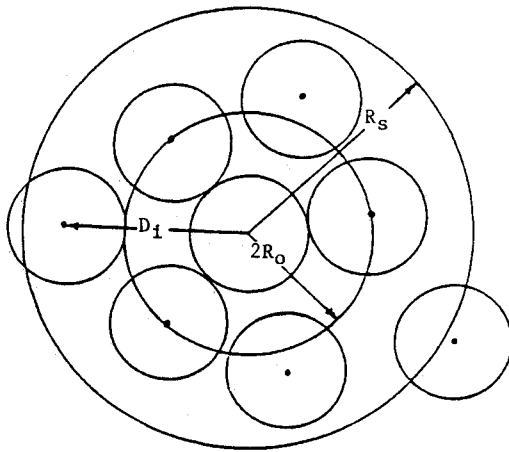


Fig. 3 Nearest-neighbor determination.

defines the maximum distance from the center node that an element may search for nearest neighbors and becomes in effect a measure of the fluid cohesive strength. As the search radius increases, the time step to maintain numerical stability is reduced because the center element is able to communicate over a larger volume to other elements. The two-dimensional fluid jet impact studies show this stability dependence on the search radius.

### Fluid Jet Study

The two-dimensional fluid jet is chosen as the test vehicle to characterize the fluid element. The fluid jet is composed of water traveling at a representative velocity of 15000 in./s. An aspect ratio of 5 is given to the fluid jet in an effort to avoid end effects while being computationally economical. A planar closest-packed assemblage of fluid elements represents the fluid jet. Figure 4a shows the fluid jet model oriented at 45 deg to the rigid surface. The elements are initially all of equal volume in the closest-packed array.

The numerical stability analysis of the fluid pressure-volume relationship, Eq. (1), used in the explicit integration solution showed that the element "stiffened" with increasing deflection requiring a time-step-size reduction to maintain stability. A time-step study was employed to determine the explicit integration-stability limits. Stability is maintained if

$$\Delta t \leq 0.4 R_0 / c \quad (5)$$

Stable and unstable deflected position plots are shown in Figs. 4b and 4c. The time-step-study results also showed that the fluid jet transferred too much normal momentum to the rigid surface due to the "bounce-off" behavior of the elements. At typical impact speeds, soft-body projectiles do not exhibit this bounce-off phenomenon. To prevent the element bounce, an energy-loss mechanism based on a variable bulk modulus is introduced. The variable modulus alters  $\beta$ , between a compression modulus  $\beta_1$  and an expansion modulus  $\beta_2$ . The choice of which modulus to use is based upon the sign of the rate of change of an element radius as

$$\begin{aligned} \beta &= \beta_1 & \text{if } dR/dt \leq 0 \\ &= \beta_2 & \text{if } dR/dt > 0 \end{aligned} \quad (6)$$

The effectiveness of the variable-bulk-modulus approach is illustrated in Fig. 4d.

The fluid jet also provided the vehicle to characterize the search radius  $R_s$ . The search radius limits the distance that an element uses to locate nearest neighbors becoming, in effect, a measure of the intraelement tensile strength. As the search dis-

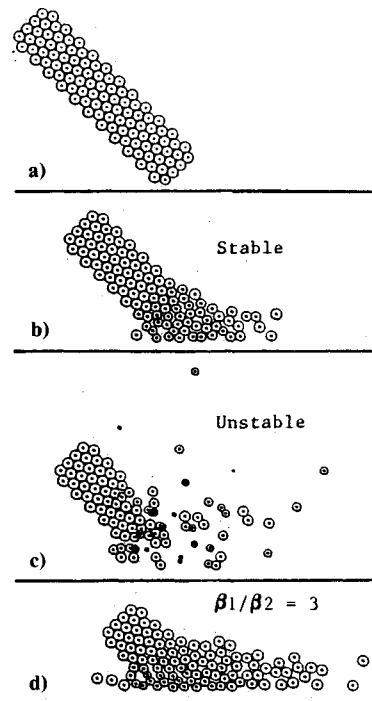


Fig. 4 Fluid jet model and deflected positions.

tance increases, the area of influence for an element increases requiring a smaller time step to maintain stability. To minimize the computational costs, the smallest possible search producing reasonable results in selected. The previous fluid jet studies for time step and bulk modulus used a search radius factor, SRF, of 1.

$$\text{SRF} = R_s / (2R_0) \quad (7)$$

Additional fluid jet analyses indicated that increasing the SRF while maintaining a constant time-step size created a run which was less stable and more expensive. The time-step estimate, Eq. (5), may be modified to incorporate the SRF destabilizing effect.

$$\Delta t < (0.45 / \text{SRF}) R_0 / c \quad (8)$$

The increased computer time required by the SRF was not justifiable based upon the results. Neither the flow pattern nor momentum transfer were significantly altered. The results obtained in all of the test cases were acceptable using an SRF = 1, which is the recommended value.

### Comparison with Test Results

The fluid FE successfully predicted the flow pattern and normal momentum transfer for the simple two-dimensional fluid jet impacts. The real test, however, was to reproduce the test results analytically. To accomplish such an analysis, the fluid FE projectile model was merged with a transient nonlinear structural analysis, WHAM,<sup>21-24</sup> to produce the PW/WHAM impact analysis. Three test cases demonstrate the PW/WHAM program capabilities: 1) a simple normal impact on a stainless steel disk, 2) a blade-like tapered flat-plate impact, and 3) a tactical fighter engine fan-blade impact.

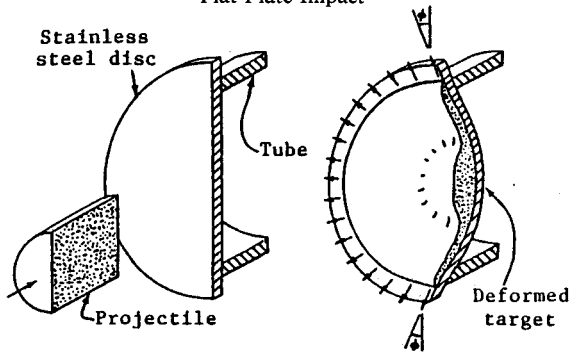
#### Stainless Steel Disk Impact

A series of impact experiments to measure the momentum transferred to pendulum-mounted targets were performed by Barber et al.<sup>27</sup> One of the tests involved an AISI 403 stainless steel disk (6.95 in. diam  $\times$  0.14 in. thick), simply supported on a 6-in.-diam cylinder, and mounted normal to the projectile

**Table 1 Stainless steel disk impact results: test vs analysis**

	Test	WHAM	Difference, %
$d$ , in.	0.57	0.56	-1.8
$\theta$ , deg	9.4	9.9	+5.3
Momentum, lb-s	4.02	4.14	+3.0

Flat-Plate Impact



trajectory. The projectile, a right circular gelatin cylinder (1.732 in. diam  $\times$  1.732 in. height) with a specific gravity of 1.0, was fired from a pressurized cannon at a velocity of 8582.7 in./s normal to the disk center.

The projectile model consisted of a closest-packed array of 228 fluid FE's. Each element had an initial radius of 0.144 in. The structural model of the 403 stainless steel disk consisted of constant strain triangular elements. The entire model was treated as a nonlinear region with the appropriate strain-rate-sensitive stress-strain law input. A viscous damping was applied to the structural model following the projectile impact in order to speed up the formation of a final deflected shape.

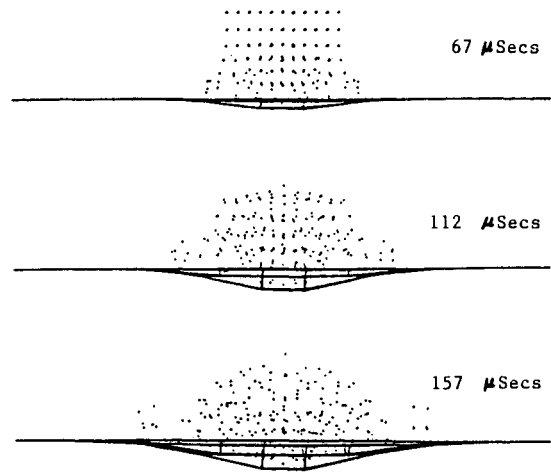
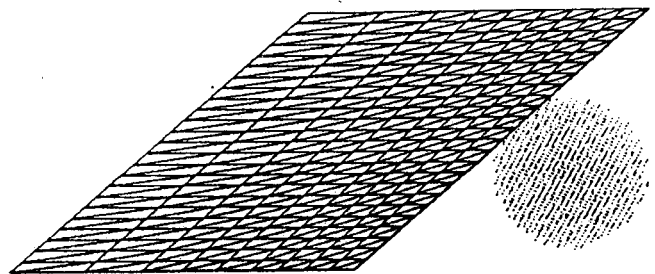
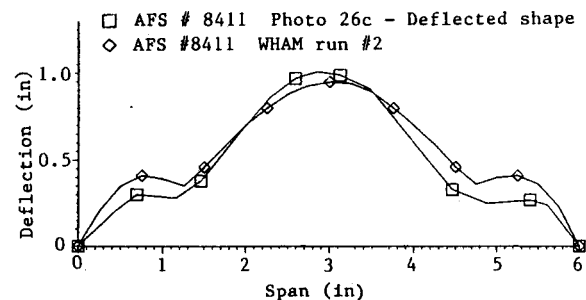
Comparison of the test data and analysis results listed in Table 1 show excellent agreement. A sampling of the outermost fluid elements velocity after impact revealed an increased velocity of approximately 60% over the initial normal velocity. This was consistent with the fluid jet studies. Figure 5 follows the impact even through time showing the projectile-structure interaction. The program which generated these plots connects the deformed nodal points on the disk with straight lines, explaining the flat surfaces.

#### Flat-Plate Impact

The fluid finite element was initially developed to fill the need for an interactive soft-body loading model for turbofan engine fan-blade impact analyses. The two-dimensional fluid jet impact studies and the stainless disk impact did not demonstrate all of the capabilities required to simulate the fan-blade impact event. A fan-blade impact, in general, cuts the projectile into two or more pieces while undergoing large deflections.

To demonstrate these capabilities, an impact on a titanium flat plate was analyzed. Impact studies performed by Bertke and Barber<sup>28</sup> on tapered leading-edge flat-plate specimens provided the ideal test case. The goal of the test program was to determine what experimental techniques and geometries would best simulate actual fan-blade impacts. Specimen mounting, leading-edge geometry, impact velocity, impact angle, projectile size, and density were the variables considered in the tests. The damage was characterized by dent size, dent shape, and leading-edge strain. The test results verified that flat plates with tapered leading edges sustained damage similar to actual fan blades subjected to soft-body impacts.

The FE modeling of the 6  $\times$  3-in. titanium plate was similar to the disk model. Constant strain triangular elements, assembled in Fig. 6, and a strain-rate-sensitive material law were input to the transient nonlinear structural analysis. The breakup is leading-edge biased to best model the 4 deg taper from a 0.020 in. leading edge to constant thickness of 0.067 in. The 1.25-in.-diam microballoon gelatin projectile (specific gravity = 0.69) was represented by 1516 fluid elements. The micro-

**Fig. 5 Side view of the projectile-disk interaction.****Fig. 6 Titanium flat-plate finite-element model.****Fig. 7 Flat-plate leading-edge normal deflection.**

balloon gelatin is a common substitute for birds in impact studies. As in the previous cases, the SRF was set at 1 with a bulk modulus ratio of 3.

Test results showed a double-dent deflection pattern on the leading edge indicating the impact was too severe for the 6-in. specimen length. The deflected leading-edge projection was estimated from a photograph in the report and plotted in Fig. 7. Superimposed is the analysis predicted shape obtained by applying a viscous damping after the projectile impact was completed. The comparison of analytically predicted leading-edge strain, deflection, and impacting mass to test results shows good agreement (Table 2). Figure 8 shows the projectile being cut by the leading edge of the deforming flat plate through several time intervals. Notice how the leading edge climbs into the projectile as it deforms ingesting more mass at increasing impact angles. This behavior is typical of fan-blade impact response.

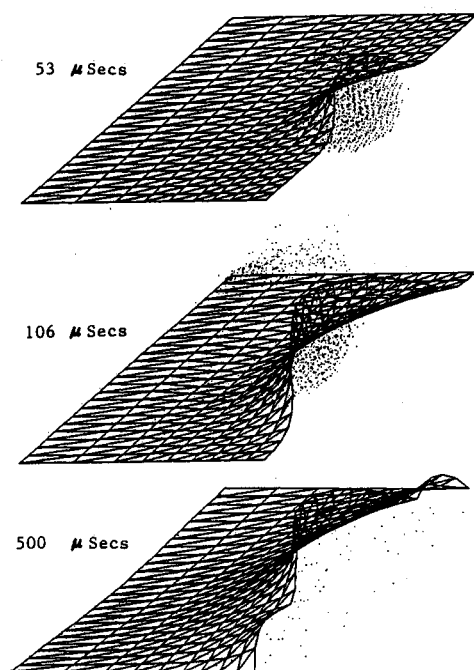


Fig. 8 The plate-projectile interaction.

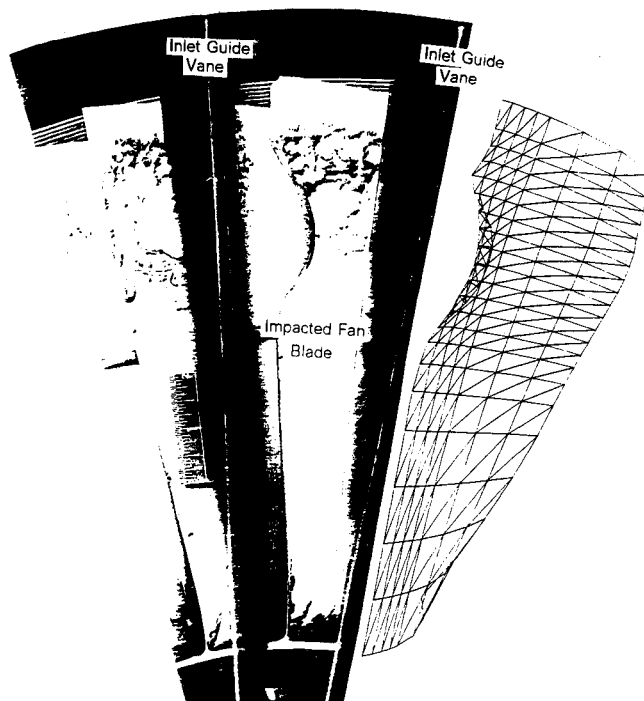


Fig. 9 Fan-blade test and PW/WHAM prediction.

Table 2 Flat-plate impact results: test vs analysis

	Test	WHAM	Difference, %
Leading-edge deflection, in.	1.03	0.95	-7.8
Leading-edge % strain	12	13	+8.3
Impacting mass, oz	0.28	0.24	-14.3

#### Fan-Blade Impact

The final demonstration involves simulation of a tactical fighter engine first-stage fan-blade bird impact. The impact data was obtained from an engine certification test in which the engine ingested a volley of 16 2-4 oz birds and continued to produce acceptable power for a given time period thereby satisfying the certification requirement. The birds, aimed to impact various spanwise locations, were shot from axial-oriented cannons into the engine. Each of the 16 birds impacts 4-5 blades imparting various levels of damage. The PW/WHAM simulation was for the first of four impacted blades at a 70% span radius. The blade preceding the analysis blade had bird markings but no damage indicating that the blade of interest sustained a maximum slice impact.

The blade FE model rotates during the impact as the bird model translates in the axial direction. In order to condition the blade for rotation efficiently, a static analysis generated deflection vector is prescribed. The blade root and shroud are constrained to rotate at the specified speed while all of the remaining nodes are given the appropriate initial velocity and acceleration. The prescribed deflection vector and specified initial conditions place the blade in equilibrium prior to impact. The bird, modeled as a prolate spheroid, is axially positioned to produce a maximum thickness slice, similar to the test condition and given an initial axial velocity equal to the bird velocity measured in the test. The bird-model axial length is reduced to include only the impact slice and sufficient additional length to avoid end effects in order to reduce computer time. The modeling and impact conditions are shown in Table 3.

The blade damage was limited to a 3.5 in. spanwise by 0.8 in. out-of-plane dent with no cracking or material loss experienced. The PW/WHAM analysis-predicted dent agrees well with the test (Fig. 9). The crack-prediction parameter value, ratio of the maximum leading-edge strain to failure strain, of

Table 3 Modeling and impact condition

Blade model, number of elements	294
Blade model, number of nodes	176
Bird model, number of elements	1751
Impact angle, deg	25
Relative velocity, ft/s	1321
Maximum slice, in.	0.7
Time step, $\mu$ s	0.25
Number of steps	2000

0.9 indicates no expected cracking, again consistent with test. The chordwise dent gradient match between test and analysis clearly shows the fluid FE projectile ability to dynamically interact with the deforming structure in a realistic manner.

#### Conclusions

A transient, material and geometric nonlinear, FE-based impact analysis, PW/WHAM, has been presented. The fluid FE formulation, reflecting an engineering approach to the complicated response of a soft-body projectile during an impact event, was introduced. The fluid-element formulation is based on the assumption that a gross momentum transfer governs the impact event. The fluid FE projectile model generates an approximate spatial and temporal load distribution. Predicting the projectiles, internal pressures, or the microfluid response is left to other techniques, such as the particle and cell analysis. Correlation with the test data covering a wide range of applications verify the assumptions used in the development of the fluid element.

The PW/WHAM, the combination of the WHAM program and the fluid FE soft-body loading model, gives the analyst a tool which can be used to design impact resistant components. The design tool, unlike experience-based tools, is not problem dependent and can be applied to most structural components concerned with impact damage from soft bodies. The FE technique, by its nature, is easily applied to new structural design concepts. This versatility is required if new designs are to be evaluated for structural requirements such as foreign-object damage.

## References

- <sup>1</sup>Hopkins, H. G. and Kolsky, H., "Mechanics of Hypervelocity Impact of Solids," *Proceedings of the Fourth Symposium on Hypervelocity Impact*, Air Force Proving Ground Center, Eglin AFB, Florida, Paper No. 12, 1960.
- <sup>2</sup>Allcock, A. W. R. and Collin, D. M., "The Development of a Dummy Bird for Use in Bird Strike Research," U.D.C. No. 598.2:621-757, June 1968.
- <sup>3</sup>Barber, J. P., Taylor, H. R., and Wilbeck, J. S., "Characterization of Bird Impacts on a Rigid Plate, Pt. 1," Air Force Flight Dynamics Lab., Wright-Patterson AFB, OH, AFFDL-TR-75-5, Jan. 1975.
- <sup>4</sup>Peterson, R. L. and Barber, J. P., "Bird Impact Forces in Aircraft Windshield Design," Air Force Flight Dynamics Lab., Wright-Patterson AFB, OH, AFFDL-TR-75-150, March 1976.
- <sup>5</sup>Barber, J. P., Taylor, H. R., and Wilbeck, J. S., "Bird Impact Forces and Pressures on Rigid and Compliant Targets," Air Force Materials Lab., Wright-Patterson AFB, OH, AFML-TR-77-60, May 1977.
- <sup>6</sup>Barber, J. P., Fry, P. F., Klyce, J. M., and Taylor, H. R., "Impact of Soft Bodies on Jet Engine Fan Blades," Air Force Materials Lab., Wright-Patterson AFB, OH, AFML-TR-77-29, April 1977.
- <sup>7</sup>Tsai, S. W., Sun, C. T., Hopkins, A. K., Hahn, H. T., and Lee, T. W., "Behavior of Cantilevered Beams Under Impact by a Soft Projectile," Air Force Materials Lab., Wright-Patterson AFB, OH, AFML-TR-74-94, Nov. 1974.
- <sup>8</sup>Cornell, R. W., "Elementary Three-Dimensional Interactive Rotor Blade Impact Analysis," *ASME Engineering for Power*, Vol. 98, No. 4, Oct. 1976.
- <sup>9</sup>Wong, T., and Cornell, R. W., "Test Methodology Correlation for Foreign Object Damage," Air Force Materials Lab., Wright-Patterson AFB, OH, AFML-TR-78-16, March 1978.
- <sup>10</sup>Fulton, G. B., "Design and Qualification of Foreign-Object Damage Resistant Turbofan Blades," AIAA 1975.
- <sup>11</sup>Constantino, C. J., "Finite-Element Approach to Stress Wave Problems," *Journal of Engineering Mechanics Division, ASCE*, Vol. 93, 1967, pp. 153-166.
- <sup>12</sup>Wilson, E. L., "A Computer Program for the Dynamic Stress Analysis of Underground Structures," Rept. to Waterways Experimental Station, U. S. Army Corps. of Engineers, Univ. of Calif., Berkeley, CA, Rept. 68-1, 1968.
- <sup>13</sup>Haisler, W. E., Jr., "Development and Evaluation of Solution Procedures for Nonlinear Structural Analysis," Ph.D. Thesis, Texas A&M Univ., College Station, TX, 1970.
- <sup>14</sup>Stricklin, J. A., Haisler, W. E., and Riesemann, W. A., "Computation and Solution Procedure for Nonlinear Analysis by Combined Finite-Element—Finite-Difference Methods," National Symposium on Computer, Structural Analysis, and Design, George Washington Univ., Washington, DC, March 1972.
- <sup>15</sup>Oden, J. T., "Finite-Element Application in Linear and Nonlinear Thermo-Viscoelasticity," EMD Specialty Conference, American Society of Civil Engineers, New York, 1967.
- <sup>16</sup>Oden, J. T., *Finite Elements of Nonlinear Continua*, McGraw-Hill, New York, 1972.
- <sup>17</sup>Wu, E. H., and Witmer, E. A., "Finite-Element Analysis of Large Plastic Transient Deformations of Simple Structures," *AIAA Journal*, Vol. 9, 1971.
- <sup>18</sup>Bathe, K., Ramm, E., and Wilson, E. L., "Finite-Element Formulations for Large Deformation Dynamic Analysis," *International Journal for Numerical Methods in Engineering*, Vol. 9, 1975.
- <sup>19</sup>Bathe, K., and Ozdemir, H., "Elastic-Plastic Large Deformation Static and Dynamic Analysis," *Computers and Structures*, Vol. 6, 1976.
- <sup>20</sup>Krieg, R. D., and Key, S. W., "Transient Shell Response by Numerical Time Integration," *International Journal for Numerical Methods in Engineering*, Vol. 7, 1973.
- <sup>21</sup>Belytschko, T. B., and Hsieh, B. J., "Nonlinear Transient Finite-Element Analysis With Convected Coordinates," *International Journal for Numerical Methods in Engineering*, Vol. 7, 1973, pp. 255-272.
- <sup>22</sup>Belytschko, T. B., and Hsieh, B. J., "Nonlinear Transient Analysis of Shells and Solids of Revolution by Convected Coordinates," AIAA Paper 73-359, 1973.
- <sup>23</sup>Belytschko, T. B., and Marchertas, A. H., "Nonlinear Finite-Element Method for Plates and Its Application to Dynamic Response of Reactor Fuel Subassemblies," American Society of Mechanical Engineers, New York, ASME Paper 74-NE-10.
- <sup>24</sup>Belytschko, T. B., Chiapetta, R. L., and Bartel, H. D., "Efficient Large-Scale Nonlinear Transient Analysis by Finite Elements," *International Journal for Numerical Methods in Engineering*, Vol. 10, 1976, pp. 579-596.
- <sup>25</sup>Martin, N. F., "A Fluid Finite-Element Soft-Body Projectile Model for Impact Damage Analysis," Masters Thesis, Univ. of Delaware, Newark, DE, June 1982.
- <sup>26</sup>Plapp, J. E., *Engineering Fluid Mechanics*, Prentice Hall, Englewood Cliffs, NJ, 1968.
- <sup>27</sup>Barber, J. P., Fry, P. F., Klyce, J. M., and Taylor, H. R., "Impact of Soft Bodies on Jet Engine Fan Blades," Air Force Materials Lab., Wright-Patterson AFB, OH, April 1977.
- <sup>28</sup>Bertke, R. S., and Barber, J. P., "Impact Damage in Titanium Leading Edges from Small Soft-Body Objects," Air Force Materials Lab., Wright-Patterson AFB, OH, AFML-TR-79-4019, March 1979.